ACS OMEGA

http://pubs.acs.org/journal/acsodf

Article

Molecular Simulation Study on the Density Behavior of *n*-Alkane/CO_2 Systems

Youhui Wang, Yulong Chen,* Junliang Wang,* Zhiyan Pan, and Jun Liu

Cite This: *ACS Omega* 2021, 6, 29618−29628

Read Online

ACCESS | Metrics & More | Article Recommendations | Supporting Information

ABSTRACT: The density and volumetric behavior of three typical *n*-alkanes (hexane, octane, and decane) influenced by different mole fractions of CO_2 injected in them at temperatures from 303 to 363 K and pressures from 3.8 to 8.67 MPa were investigated by performing molecular dynamics simulations. It is shown that the mass density first increases and then decreases with increasing CO_2 mole fraction. Correspondingly, the system volume only slightly swells at low CO_2 contents while suddenly expanding when the CO_2 mole fraction exceeds a value of ∼60%. The calculations of structural properties and interaction energies indicate that at low CO_2 mole fractions, there are a few CO_2 molecules existing in the gap of alkane molecules, resulting in poor compressibility, while at higher CO_2 concentrations, the CO_2 molecules begin to separate from the CO_2-saturated alkane phase and form a gas phase, leading to higher compressibility. Therefore, at high CO_2 mole fractions, the system density and volume can more easily be changed by temperature and pressure than that at low CO_2 mole fractions. In addition, since it is harder for alkanes with longer chains to separate from each other, the volume swelling decreases and the density increases with increasing carbon number of *n*-alkane chains. Finally, we found that the increase in CO_2 mole fraction, temperature, and the decrease in alkane chain length would promote the diffusion of both CO_2 and alkane molecules. However, the influence of pressure on molecular diffusion is very limited except when P = 8.67 MPa and T = 333 K, where CO_2 is in the supercritical state. This work is helpful for understanding the density and volumetric behavior of *n*-alkane/CO_2 mixtures at a molecular level and provides useful information for guiding carbon sequestration and CO_2-enhanced oil recovery.

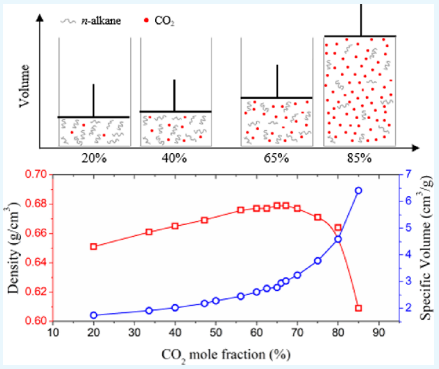

1. INTRODUCTION

Over the past 200 years, trillions of tons of anthropogenic carbon dioxide (CO_2), mainly from the combustion of fossil fuels, have been emitted into the atmosphere, which plays a key role in global warming and leads to serious environmental problems.[1,2] Only between 1901 and 2010, the global warming resulted in a 20 cm increase in the global mean sea level.[3] To mitigate severe events of climate change, many countries have proposed plans to achieve the goals of carbon emission peak and carbon neutrality in the coming decades.[4]

Carbon capture and storage (CCS), i.e., capture of CO_2 from exhaust gases, followed by storing it in an appropriate natural reservoir, is an important solution for the reduction of anthropogenic CO_2 emissions.[5−9] Injection of CO_2 into oil-bearing reservoirs is one of the most promising options that not only can reduce CO_2 accumulation in the atmosphere but also can improve oil recovery.[10−13] Specifically, this technology can sequestrate 60% of the injected CO_2 underground and can enhance oil recovery by 10−15%.[14] As CO_2 is injected into an oil-bearing reservoir, it will dissolve in the crude oil and can change the thermodynamic properties of the mixture, such as density, volume, and phase, which are crucial for fluid diffusion and migration.[15−21] Therefore, the variation of oil properties after injecting CO_2 needs to be sufficiently understood for ensuring the safety and efficiency of the CO_2-enhanced oil recovery (EOR) projects.

Many experiments focusing on the density and swelling effect of alkane/CO_2 systems have been carried out.[21−30] A very recent review study by Zhao et al.[22] summarized that the saturated and compressed-liquid densities of decane/CO_2 solutions have been measured comprehensively with temperatures reaching 510.9 K and pressures up to 76.4 MPa. However, density data for other alkane/CO_2 systems are limited to a certain range of pressure and temperature at the phase-equilibrium and compressed-liquid states. The measurement of the density near the supercritical state of the alkane/CO_2 solutions remains a big challenge. Simultaneously, experimental studies are often costly and time-consuming and cannot gain information from a microscopic perspective. Although various models and correlations have been developed

Received: July 21, 2021
Accepted: October 20, 2021
Published: October 29, 2021

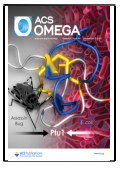

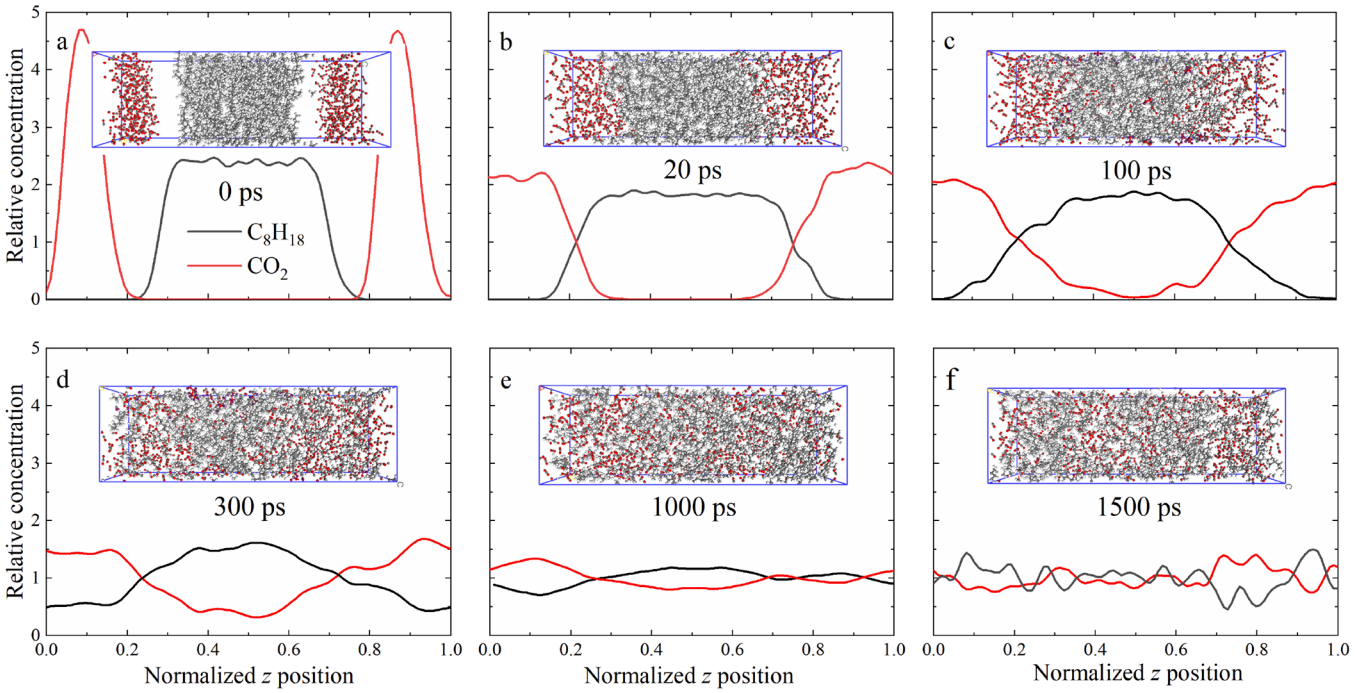

Figure 1. Temporal evolution of relative concentrations of C_8H_{18} (black) and CO_2 (red) along the z axis for an initially phase-separated octane/CO_2 system under an NPT ensemble at P = 7.69 MPa and T = 333 K: (a) t = 0, (b) 20, (c) 100, (d) 300, (e) 1000, and (f) 1500 ps. The insets show the corresponding simulation snapshots.

to predict the thermodynamic properties of the alkane/CO_2 systems under specific conditions, the prediction ability and generality still need to be verified and improved.[22]

With the progress in computing technology, molecular simulation methods, such as Monte Carlo (MC) and molecular dynamics (MD), have attracted increasing attention in studying the behavior of gas/liquid mixtures, which potentially allow for significantly shorter turnaround times and microscopic insights into the system. Using molecular simulation approaches, attempts have been made to understand the solubility and diffusivity of CO_2 in various alkanes,[31−33] the interfacial property,[34−37] phase equilibrium,[37,38] volume swelling,[33,39,40] and the reduction in viscosity[40] of the alkane/CO_2 systems. Liu et al.[39] investigated the effects of temperature, pressure, and alkane structure on the volume swelling of CO_2-saturated alkanes (decane, octane, hexane, and cyclohexane) by performing MD simulations. In their work, the solubility of CO_2 in the alkanes was taken from experimental data. Zhang et al.[33] calculated the CO_2 solubility in octane and investigated its effect on octane by means of configurational-bias MC simulations in the osmotic ensemble, showing that the interaction between octane and CO_2 is the main cause of the octane swelling. By combining MD and configurational-bias MC simulations, Li et al.[40] studied the effects of alkane chain length, pressure, and temperature on the CO_2 solubility, volume swelling, and viscosity reduction of CO_2/n-alkane (octane, decane, dodecane, tetradecane, and hexadecane) systems. Very recently, Zhang et al.[32] also used a combined MC and MD simulation approach to investigate the CO_2 solubility in two well-known alkanes named decane and n-eicosane and to understand the effect of CO_2 solubility on the density, specific volume, swelling, static structure, diffusion, and viscosity of CO_2-saturated alkanes.

As illustrated above, despite the fact that fruitful insights have been achieved, most of the published molecular simulation works only focused on the volume swelling of CO_2-saturated alkanes. Minimum efforts were allocated to investigate the volumetric behavior of alkane/CO_2 systems influenced by different mole fractions of CO_2. Moreover, there are also a few simulations concentrating on the change in oil phase density after injecting CO_2 since it may not look like an oil recovery mechanism compared to oil viscosity reduction and oil swelling. However, many previous experimental studies have shown that the density of alkane/CO_2 mixtures first increases with increasing CO_2 mole fraction but decreases at higher CO_2 concentrations and higher temperatures.[21,25−28] An increase in oil phase density should result in an increase in gravitational forces acting on oil ganglia, which is favorable for gravity-assisted gas injection scenarios because higher gravitational forces could lead to drainage of oil through the oil layer present in the cervices of pores and their reconnection and production.[32]

Therefore, in this work, the density and volumetric behavior of three typical n-alkanes (hexane, octane, and decane) influenced by different mole fractions of CO_2 injected in them were systematically investigated by means of all-atom MD simulations. The ranges of temperature and pressure studied are from 303 to 363 K and from 3.8 to 8.67 MPa, respectively, corresponding to the reservoir conditions of oils at depths of around 1−3 km.[33] To understand the underlying microscopic mechanism, the conformation, packing structure, and interaction energy between molecules were also analyzed. Finally, the influences of density and volumetric behavior on the molecular diffusion of CO_2 and alkanes were also investigated since it is directly correlated with carbon sequestration and oil recovery. The study on alkane density change at a molecular level would assist in evaluating the effect of CO_2 on the underground hydrocarbon recovery and the environmental safety for CO_2 storage.

https://doi.org/10.1021/acsomega.1c03889
ACS Omega 2021, 6, 29618−29628

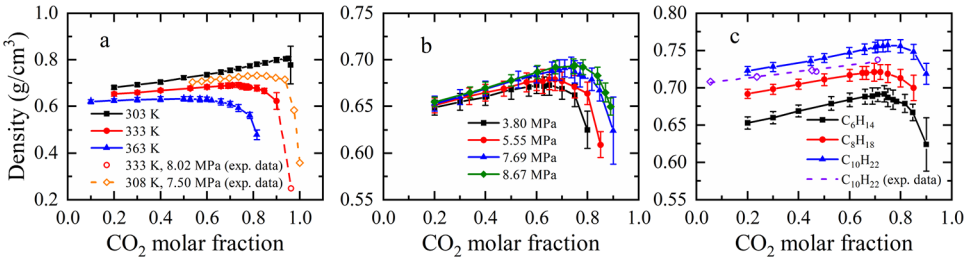

Figure 2. Density of the hexane/CO_2 system as a function of CO_2 mole fraction: (a) at a fixed pressure P = 7.69 MPa but at different temperatures and (b) at a fixed temperature T = 333 K but at different P values as indicated. (c) Densities of different n-alkane/CO_2 systems as a function of CO_2 mole fraction at P = 7.69 MPa and T = 333 K. The red open circles and the orange open diamonds in panel (a) represent experimental data taken from Wang et al.[29] at T = 333 K and P = 8.08 MPa and from Tolley et al.[30] at T = 308 K and P = 7.50 MPa, respectively. The violet open circles and diamonds in panel (c) represent the density data of decane/CO_2 systems at T = 333 K and P = 8 MPa taken from Zúñiga-Moreno et al.[28] and Song et al.,[26] respectively.

2. SIMULATION DETAILS

We used the Materials Studio software package for carrying out the all-atom MD simulations. The condensed-phase optimized molecular potential for atomistic simulation studies (COMPASS) force field, a widely used all-atom force field based on ab initio calculation and optimization by experimental data, was applied to describe all the potentials, including the bonded and nonbonded potentials, of CO_2 and alkane molecules. It has been validated that the COMPASS force field can accurately predict structural and thermophysical properties for a broad range of organic and inorganic substances including CO_2 and alkanes.[41−43]

The total potential energy was described by

$$U = U_{\text{bond}} + U_{\text{angle}} + U_{\text{dihedral}} + U_{\text{improper}} + U_{\text{cross}} + U_{\text{vdW}} + U_{\text{Coulomb}} \quad (1)$$

where the first five terms on the right side of the equation are the bonded potentials, corresponding to bond stretching, angular bending, dihedral angle torsion, out-of-plane interactions, and their cross-coupling term, respectively, while the last two terms are the nonbonded potentials, i.e., the short-range van der Waals (vdW) and the long-range Coulomb interactions, respectively. The vdW interactions were described by Lennard-Jones (LJ) 9−6 potentials expressed as

$$U_{\text{vdW}}(r) = \varepsilon\left[2\left(\frac{\sigma}{r}\right)^9 - 3\left(\frac{\sigma}{r}\right)^6\right] \qquad \text{for } r < r_c \quad (2)$$

where ε is the depth of the potential well, σ is the LJ size, r is the separation distance between a pair of atoms, and r_c is the cutoff distance that was introduced to exclude energy and force computations if separation between atoms is over this cutoff value. We used a truncated and shifted potential with a cutoff of 12.5 Å. The Coulomb interactions in the system were calculated using Ewald summation, which is given by

$$U_{\text{Coulomb}}(r) = C\frac{q_i q_j}{\epsilon r} \quad (3)$$

where C = 332.0637 (kcal/mol) Å/e^2 is the unit conversion factor, q_i and q_j are the partial charges of the pair atoms i and j, respectively, and ϵ = 1 is the relative dielectric constant.

Initially, a system consisting of two independent bulk phases of alkane (hexane, octane, or decane) and CO_2 was constructed. The number of alkane molecules was fixed at 150, while the number of CO_2 was varied for investigating the influence of CO_2 mole fraction on alkane. The binary systems were subjected to three-dimensional periodic boundary conditions. The original configuration of a CO_2/octane binary system is depicted in Figure 1a. At first, energy minimization was performed for each system using a smart minimizer approach. Following the minimization, isothermal−isobaric (NPT) simulation was carried out to compress the system and to equilibrate the structures for at least 1.5 ns with a time step of 1 fs. The temperatures and pressures of the systems were controlled at 303−363 K by the Andersen thermostat and at 3.8−8.67 MPa by the Berendsen barostat, respectively. The changes in configuration, density, and energy were monitored (Figure S1) for examining whether the system has reached equilibrium. After equilibration, the average values of the properties we are interested in were calculated. The qualities like density, specific volume, and diffusion coefficients of CO_2 and alkanes for different systems are tabulated in Table S1 in the Supporting Information and will be discussed in detail in the following section.

3. RESULTS AND DISCUSSION

3.1. Microscopic Process of CO_2 Dissolving in an Alkane. To observe the microscopic CO_2 dissolving process, taking the initially phase-separated octane/CO_2 system as an example, the temporal evolution of the relative concentrations of octane and CO_2 along the z axis during an NPT run was monitored. The results are presented in Figure 1, where the corresponding simulation snapshots are also included for intuitive observations. Figure 1a shows that, initially, the octane and CO_2 molecules are phase-separated with the octane phase located in the middle of the simulation box along the z dimension. Between the two phases, there are free spaces available for molecules to occupy. At t = 20 ps, the spaces between the octane and CO_2 phases are occupied by CO_2 molecules, and some CO_2 molecules even begin to penetrate to the octane phase, leading to a slight swelling of the octane volume (Figure 1b). As the simulation proceeds, more CO_2 molecules diffuse into octane and some octane molecules also diffuse into the CO_2 phase (Figure 1c). In this stage, the CO_2 molecules that entered the octane phase still gather in the form of small groups rather than separating from each other. These CO_2 groups would divide the octane phase into many small clusters (Figure 1d). Consequently, octane swells further, offering more spaces for CO_2 to diffuse. As CO_2 molecules continuously penetrate to the octane clusters, the clusters are further divided into much smaller clusters or even single

https://doi.org/10.1021/acsomega.1c03889
ACS Omega 2021, 6, 29618−29628

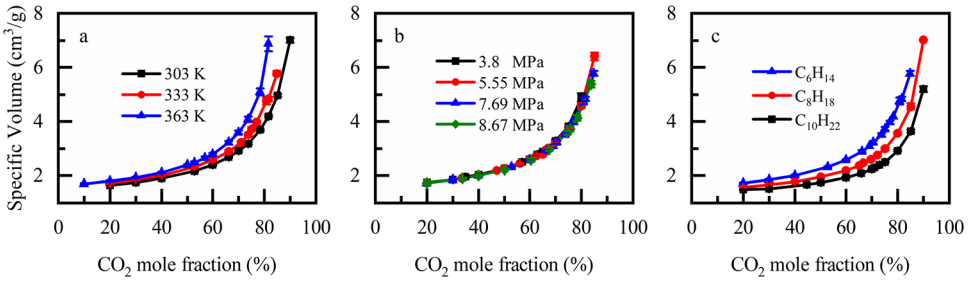

Figure 3. Specific volume of CO_2-mixed hexane, defined as cubic centimeters occupied by 1 g of alkane, as a function of CO_2 mole fraction: (a) at a fixed P = 7.69 MPa but at different T values and (b) at a fixed T = 333 K but at different P values as indicated. (c) Specific volumes of CO_2-mixed hexane, octane, and decane as a function of CO_2 mole fraction at P = 7.69 MPa and T = 333 K.

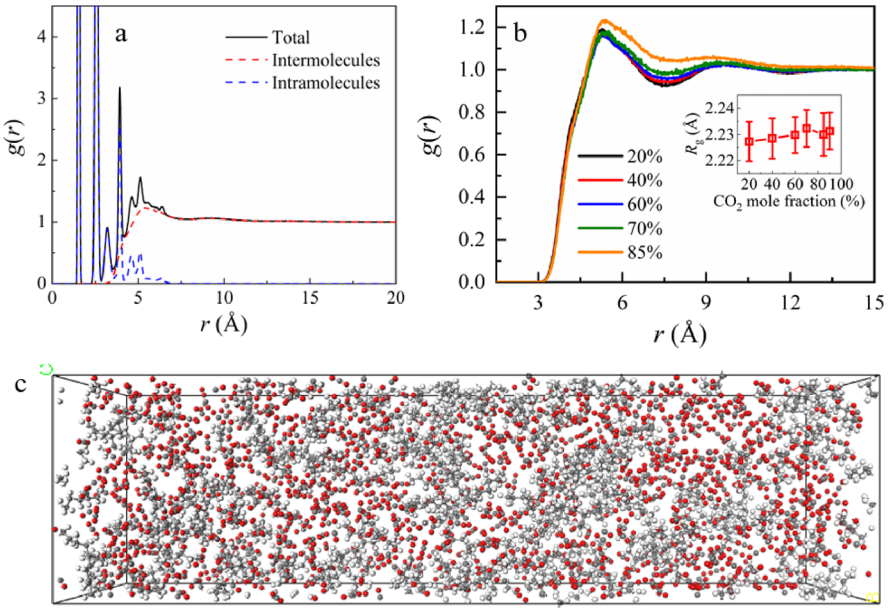

Figure 4. (a) Radial distribution function (RDF) of carbon atoms of hexane molecules and their inter- and intramolecular parts, as indicated, for the hexane/CO_2 system with 85% CO_2 mole fraction. (b) RDFs of the intermolecular carbon atoms of hexane in systems with varied CO_2 mole fractions. The inset shows the radius of gyration of alkane chains. (c) Typical snapshot of the hexane/CO_2 system with 85% CO_2 mole fraction. The results are obtained at P = 7.69 MPa and T = 333 K.

molecules (Figure 1e). Finally, the CO_2/octane system reaches the equilibrium state (Figure 1f).

3.2. Densities of *n*-Alkane/CO_2 Systems. After equilibration, the system densities were calculated. Note that, here, the quantity "density" refers to "mass density". The results are presented in Table S1 in the Supporting Information and are plotted in Figure 2, where some selected literature data are also included for comparison. For a fixed composition, the density of the binary mixture decreases with temperature at a constant pressure (Figure 2a) but increases with pressure at a constant temperature (Figure 2b). When the CO_2 mole fraction is low, the density only slightly changes with temperature and pressure. However, when the CO_2 mole fraction is higher than 60% or greater, the simulated density decreases with temperature or increases with pressure more sharply, consistent with the phenomena observed by previous experimental studies.[21,25−28]

Meanwhile, we also find that with increasing CO_2 mole fraction, the mixture density first increases and then decreases (Figure 2). The CO_2 mole fraction at which the density reaches the maximum is observed to reduce with the increase in temperature (Figure 2a) but slightly increase with increasing pressure (Figure 2b). This peculiar density behavior has also been found in many previous studies.[21,25−28,30] Under similar conditions, the densities obtained from the present simulation study are in good agreement with the experimental data from Wang et al.,[29] Tolley et al.,[30] Zúñiga-Moreno et al.,[28] and Song et al.[26] The results from Tolley et al.[30] are located between the black and red curves of Figure 2a, further suggesting a lower density of hexane/CO_2 mixture with increasing temperature or decreasing pressure.

The densities of alkane/CO_2 mixtures for alkanes with different carbon numbers were also compared, as shown in Figure 2c. For the entire range of CO_2 mole fraction investigated, the densities increase with increasing carbon number because a higher carbon number can result in a higher carbon/hydrogen ratio and a lower free volume between molecules, leading to a higher mass density. Moreover, for a given alkane, the density first increases and then decreases with increasing CO_2 mole fraction and the mole fraction of CO_2 at which the density reaches the maximum increases only very slightly with the carbon number of alkane chains.

3.3. Specific Volumes of *n*-Alkanes in the *n*-Alkane/CO_2 Systems. To quantify the oil swelling effect as a result of CO_2 injection, the specific volumes of CO_2-dissolved or mixed alkanes were calculated, where the specific volume is defined as

https://doi.org/10.1021/acsomega.1c03889
ACS Omega 2021, 6, 29618−29628

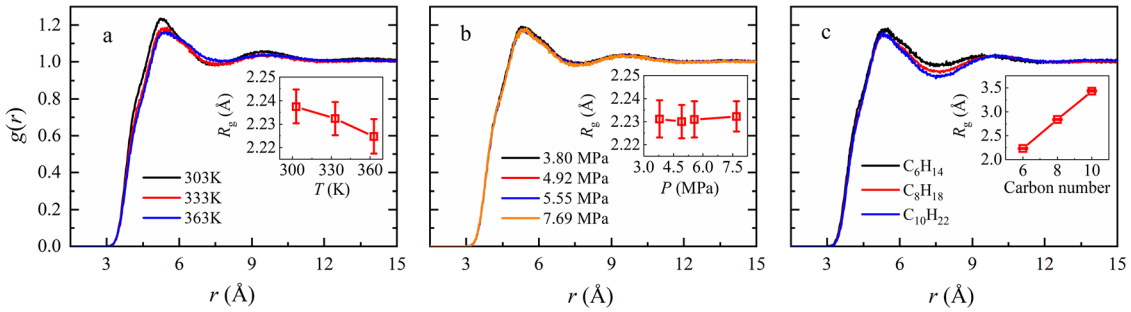

Figure 5. RDFs of the intermolecular carbon atoms of hexane in systems with 70% CO_2 mole fraction (a) at P = 7.69 MPa but at different T values and (b) at T = 333 MPa but at different P values. (c) RDFs of the intermolecular carbon atoms of hexane, octane, and decane in systems with 70% CO_2 mole fraction at T = 333 MPa and P = 7.69 MPa. The insets show the radius of gyration of alkane chains of the corresponding systems.

cubic centimeters occupied by 1 g of alkane.[32] The results are displayed in Table S1 and as well in Figure 3. From Figure 3, we see that in all cases, the specific volumes increase slowly with CO_2 mole fraction first while rising steeply when the CO_2 mole fraction exceeds a value of ~60%. At a constant pressure, the specific volumes of the binary mixtures increase with the increase in temperature (Figure 3a). This trend is particularly significant at high CO_2 mole fractions (Figure 3a). At low CO_2 mole fractions, the CO_2 molecules are dissolved in alkanes and can be considered as a single-phase liquid. However, at high CO_2 mole fractions, the systems split into two separated phases, i.e., the CO_2-saturated alkane phase and the CO_2-dominated gas phase, as will be validated later. Therefore, as the temperature increases, the system with a high CO_2 mole fraction expands more significantly than that with a low CO_2 concentration because it contains a gas phase. However, the influence of pressure on the specific volume is not so obvious (Figure 3b), although increasing the pressure can suppress the system and enhance the dissolution of CO_2 in the alkane slightly, leading to the reduction of the system volume especially when CO_2 is rich. The volumetric behaviors of different alkane systems are similar, but at a given CO_2 mole fraction, the specific volume reduces with increasing carbon number of alkane chains (Figure 3c).

3.4. Microscopic Mechanism of the Density and Volumetric Behavior. *3.4.1. Structural Properties.* One of the advantages of MD simulation methods is the ability to obtain the microscopic information of the simulated systems, which is helpful for a better understanding of the density and volumetric behavior of alkanes after being mixed with CO_2. Here, the structural properties of alkane and CO_2 molecules were first examined.

Figure 4a provides the radial distribution function (RDF) of carbon atoms of hexane molecules and their inter- and intramolecular parts. From the figure, we observe that there are several sharp peaks at short distances, corresponding to the carbon atoms on the same molecule, including the two carbon atoms that are covalently bonded ($r \approx 1.5$ Å) and those separated by one, two, or more CH_2 groups. However, the peaks at $r \approx 5$ Å represent either of the two carbon atoms on the same chain that are separated by at least three CH_2 groups or two neighboring carbon atoms on different alkane chains. However, from the inter-RDF and intra-RDF, one can find that the contribution of neighboring carbon atoms on different alkane chains plays a dominant role when $r \approx 5$ Å.

Figure 4b shows the RDFs of the intermolecular carbon atoms and the radius of gyration of the hexane chains (inset) for systems with varying CO_2 mole fractions. At a given temperature and pressure, we find that the RDF values at around r = 5−13 Å increase with increasing CO_2 mole fraction. This trend is extremely significant at high CO_2 mole fractions. Note that the values of RDF curves reflect the local density of other atoms around a given reference atom normalized by their averaged density over the total volume. Therefore, the results shown in Figure 4b indicate the increasingly inhomogeneous distribution of alkane molecules in the systems at high CO_2 contents because the addition of CO_2 molecules would occupy or even expand the gaps between alkane molecules, leading to significant fluctuation in their density. From Figure 4c, showing a typical snapshot of the hexane/CO_2 system at a high CO_2 mole fraction of 85%, we see that part of CO_2 molecules is accumulated in some localized regions, implying that the system would split into two separated phases, i.e., the CO_2-saturated alkane phase and the CO_2-dominated gas phase. Such phase separation is independent of the system's initial state. We have examined that even starting from an initially well-mixed configuration, the system would still become phase-separated after long enough time of equilibration (Figure S2). From the inset of Figure 4b, we find that as CO_2 is injected into the system, the alkane chains slightly extend, implying that the presence of CO_2 molecules would lead to the swelling of the alkane molecules and, consequently, the system volume.

For a fixed composition, we observe that the first peak at $r \approx$ 5.3 Å and the second peak at $r \approx$ 9.6 Å seem to slightly decrease with increasing temperature (Figure 5a), indicating that the alkane molecules can disperse more homogenously at higher temperatures. However, for each alkane molecule, the chain slightly shrinks with the increase in temperature (see the inset of Figure 5a) because, at high temperatures, the alkane chains prefer to reduce their coil size to increase their conformational entropy. This chain collapsing effect may in part lead to the reduction of CO_2 solubility in alkanes. In comparison to the effect of temperature, the influence of pressure on the alkane conformation is very limited (the inset of Figure 5b). Meanwhile, the RDF curves are also in good agreement between different pressures (Figure 5b), indicating that the packing structure of alkane molecules is almost not affected by pressure, although the bulk density and the CO_2 solubility between different systems are slightly different. For the influence of alkane chain length, we find that increasing the chain carbon number would increase the radius of gyration of alkane chains (the inset of Figure 5c). The higher chain size would make the alkane molecules hard to be separated from each other and thus with a slightly more structured local structure, as reflected from Figure 5c, where the minimum at $r \approx$ 7.5 Å decreases with increasing alkane chain length.

https://doi.org/10.1021/acsomega.1c03889
ACS Omega 2021, 6, 29618−29628

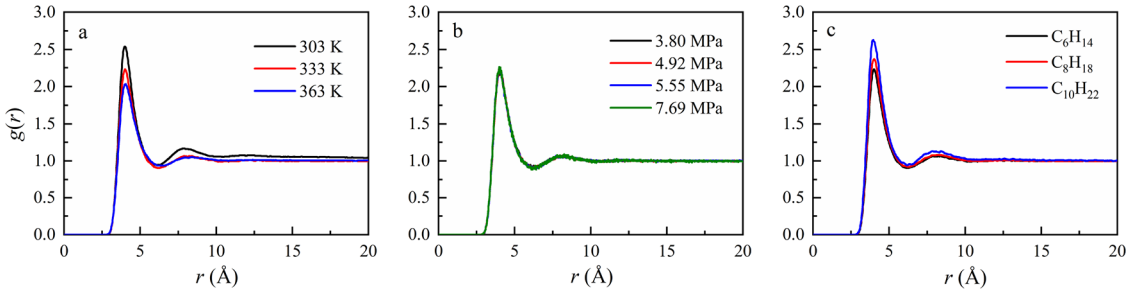

Figure 6. RDFs of carbon atoms from CO_2 molecules in hexane with 70% CO_2 mole fraction (a) at P = 7.69 MPa but at different T values and (b) at T = 333 MPa but at different P values and (c) those in hexane, octane, and decane with 70% CO_2 mole fraction at T = 333 MPa and P = 7.69 MPa.

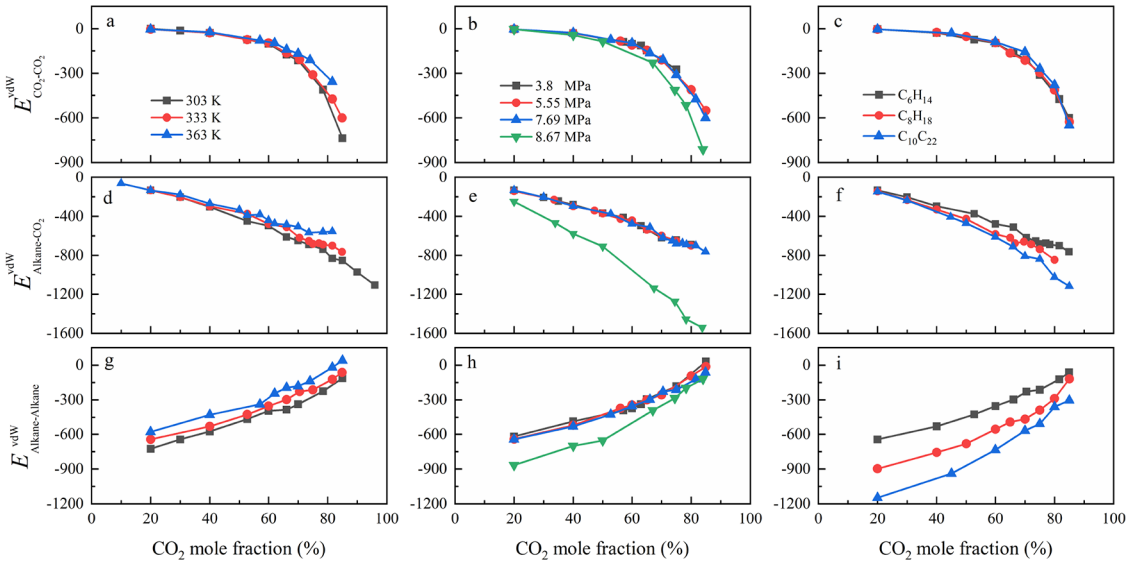

Figure 7. Van der Waals (vdW) interaction energies of (a–c) CO_2–CO_2, (d–f) alkane–CO_2, and (g–i) alkane–alkane as a function of CO_2 mole fraction in hexane/CO_2 systems (a, d, g) at a fixed P = 7.69 MPa but at different T values (b, e, h), at a fixed T = 333 K but at different P values, and (c, f, i) in systems of different n-alkanes at P = 7.69 MPa and T = 333 K.

The RDFs of carbon atoms from CO_2 molecules were also calculated, as shown in Figure 6. At short distances, the RDF curves show a zero value due to the strong repulsive forces between molecules. The first peak that appears at $r \approx 4.2$ Å is related to the most likely separation at which the two neighboring CO_2 molecules can be found. However, the second peak that occurs at around $r \approx 8$ Å corresponds to the separation of two CO_2 molecules with another CO_2 molecule inserted in between. At long distances, the RDFs approach one, which suggests that there is no long-range order in CO_2 packing. With increasing temperature, both the first and second peaks become less pronounced (Figure 6a), indicating that the CO_2 molecules become more disordered and homogeneous at higher temperatures. However, the influence of pressure on CO_2 packing is very limited (Figure 6b), consistent with the behavior of alkane molecules (Figure 5b). As the carbon number of alkane chains increases, the RDF peaks become more significant (Figure 6c) because a higher alkane molecular weight can result in harder dissolution of CO_2 in the alkane, making the CO_2 molecules with a more inhomogeneous packing structure.

3.4.2. Interaction Energy. Previous molecular simulation studies by Zhang et al.,[33] Liu et al.,[39] and Li et al.[40] argued that the interaction between CO_2 and alkane molecules is responsible for the volume swelling of alkane/CO_2 systems. Therefore, the van der Waals (vdW) interaction energies of CO_2–CO_2, alkane–CO_2, and alkane–alkane in the CO_2-mixed hexane, octane, and decane systems were also calculated, as shown in Figure 7.

We find that with increasing CO_2 mole fraction, the vdW interaction energies between CO_2 molecules become more negative (Figure 7a–c). At low CO_2 mole fractions, the CO_2–CO_2 vdW interaction energies change very slowly because the CO_2 molecules are well dissolved in the alkane phase and hence with a low probability to interact with each other. However, when the CO_2 mole fraction exceeds a value of ~60%, the interaction energies become dramatically negative, implying that at such a high CO_2 concentration, CO_2 in the alkane phase is saturated, leaving a lot of CO_2 molecules that cannot dissolve in alkane to gather as a separated gas phase. Accordingly, the volume of the mixture increases significantly (Figure 3). When the gas phase dominates the system properties, the system density decreases (Figure 2) because the density of CO_2 is lower than that of alkane at the same temperature and pressure.

As CO_2 is continuously injected, the interaction energy between alkane and CO_2 molecules becomes more negative (Figure 7d–f), while the interaction energy between alkane molecules becomes less negative (Figure 7g–i). This is due to the dissolution or penetration of more CO_2 molecules to the

https://doi.org/10.1021/acsomega.1c03889
ACS Omega 2021, 6, 29618–29628

alkane, occupying or even expanding the space between alkane molecules. In comparison to the CO_2−CO_2 interaction, the alkane−CO_2 interaction contributes a larger amount to the total interaction energy, especially when the CO_2 mole fraction is below the saturated point, suggesting that the oil swelling is predominantly controlled by the oil−CO_2 interaction.

For a given pressure, the CO_2−CO_2 and alkane−CO_2 vdW interactions are little influenced by temperature when the CO_2 mole fraction is lower than 60% (Figure 7a,d) because, at such a low CO_2 concentration, all CO_2 molecules are dissolved in the alkane. However, when the CO_2 mole fraction exceeds 60%, both the CO_2−CO_2 and alkane−CO_2 interactions become less negative with increasing temperature. The reason is that at a higher temperature, the CO_2 solubility is decreased when fewer CO_2 molecules are dissolved into the alkane, and hence, the interaction between CO_2 and alkane becomes weaker. Meanwhile, with the increase in temperature, the increasing number of undissolved CO_2 molecules that gather as a gas phase would expand, leading to a reduced negative interaction between CO_2 molecules as well. However, for the entire range of CO_2 mole fractions investigated, the alkane−alkane interaction becomes less negative with increasing temperature (Figure 7g) due to the expansion of the CO_2-satuated alkane phase.

Different from the influence of temperature, the pressure shows a very limited impact on the intramolecular vdW interactions when $P \leq 7.69$ MPa (Figure 7b,e,h). Therefore, the density and volume of the systems are only slightly affected (Figures 2b and 3b). However, when $P = 8.67$ MPa, the vdW interactions of CO_2−CO_2 (at a mole fraction > 40%), alkane−CO_2, and alkane−alkane are significantly more negative than those at lower P values, suggesting that CO_2 is in the supercritical state,[44] which can lead to significant changes in the diffusive and viscous properties of the mixtures. One should note that in the present study, the supercritical behavior of CO_2 occurred at temperature and pressure higher than that estimated from experiments, i.e., the critical temperature T_c = 304.1 K and the critical pressure P_c = 7.38 MPa in experiments.[45] This may be because the adopted COMPASS force field is not accurate enough for mimicking the behavior of alkane/CO_2 systems. In the MD study by Moultos et al.,[31] three different atomistic models were compared and it was found that the L-OPLS force field, an optimized version of OPLS, is the most accurate one to reproduce the density, viscosity, and diffusivity of CO_2 in hydrocarbons. Despite the fact that the model used in the present study is not accurate enough, it still can well describe the behavior observed in experiments (Figure 2a,c)[26,28−30] and therefore would not affect the general conclusions we obtained.

From Figure 7i, we see that the n-alkanes with a higher carbon number have a more negative intermolecular interaction energy, which means that it is harder for alkanes with longer chains to separate from each other. Meanwhile, with increasing carbon number, the alkane−CO_2 interaction energy also becomes more negative especially at high CO_2 mole fractions (Figure 7f), suggesting that longer alkane chains can lead to a denser packing of alkane and CO_2 molecules. Therefore, a higher density (Figure 2c) and a lower volume swelling (Figure 3c) can be observed when the alkane with longer chains is mixed with CO_2.

3.4.3. Microscopic Mechanism. Based on the analysis of structural and interaction properties, the microscopic mechanism of the density and volumetric behavior of n-alkane/CO_2 systems can be briefly generated as follows, as schematically shown in Figure 8. When a small amount of CO_2 is added to

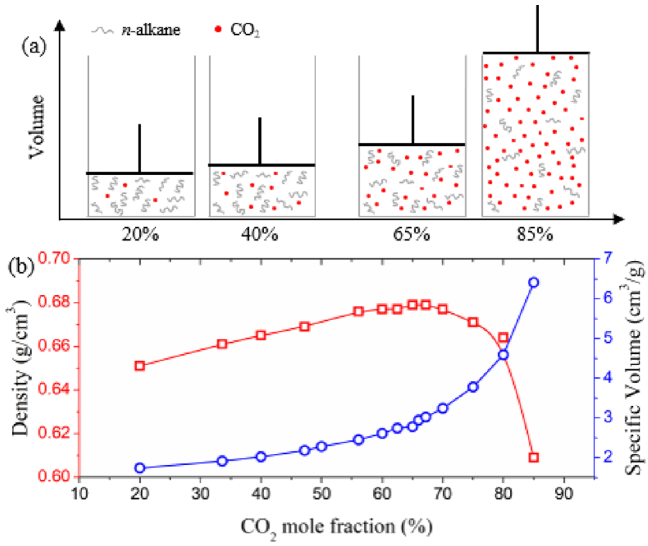

Figure 8. (a) Schematic of filling CO_2 in an n-alkane. (b) Density and hexane-specific volume of the hexane/CO_2 system as a function of CO_2 mole fraction at T = 333 K and P = 5.55 MPa.

an n-alkane, they are filled in the space between n-alkane molecules and completely dissolved in the liquid n-alkane. In this case, the alkane is only slightly swelled by CO_2 when the increase amplitude of system volume is far below that of mass, and hence, the system density increases with increasing CO_2 mole fraction. When all spaces among alkane molecules are occupied by CO_2 (at CO_2 mole fraction > 60%), the system density reaches a maximum. With further increasing the CO_2 mole fraction, the CO_2 molecules in alkane are saturated and part of them begins to separate from the alkane and form a gas phase, resulting in the rapid increase in system volume and, consequently, the reduction in density. Owing to the existence of a highly compressible gas phase at high CO_2 mole fractions, the system density and volume can more easily be changed by temperature and pressure than that at low CO_2 mole fractions. In addition, since the molecular properties and space among molecules are different between different n-alkanes, the density and volumetric behavior should also depend on the alkane properties, such as alkane chain length.

3.5. Diffusivity of CO_2 and Alkane Molecules in the Alkane/CO_2 Mixtures. It has been examined that the injection of CO_2 can significantly change the thermodynamic properties and, therefore, the diffusion and migration of crude oils, which are important for carbon sequestration and oil recovery. To design the appropriate processes of carbon sequestration and oil recovery, it is required to understand the transport property of CO_2 and alkane in the alkane/CO_2 mixtures at different temperatures, pressures, and CO_2 mole fractions. Therefore, the mean square displacements (MSDs) of CO_2 and alkane molecules were calculated, as given by[46]

$$\mathrm{MSD}(\Delta t) = \langle (\mathbf{r}_i(\Delta t) - \mathbf{r}_i(0))^2 \rangle \quad (4)$$

where $\mathbf{r}_i(\Delta t) - \mathbf{r}_i(0)$ is the distance (vector) traveled by molecule i over the time interval of Δt. The squared amplitude of this vector is averaged over different time intervals and averaged also over all CO_2 or alkane molecules. Figure 9 presents some typical MSD results of CO_2 and hexane

https://doi.org/10.1021/acsomega.1c03889
ACS Omega 2021, 6, 29618−29628

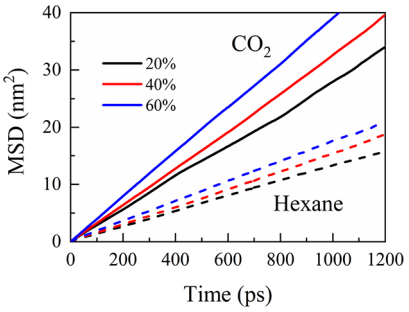

Figure 9. Mean square displacement (MSD) of CO_2 (solid) and hexane (dashed) molecules in the hexane/CO_2 mixtures with varied CO_2 mole fraction at T = 333 K and P = 7.69 MPa.

molecules in the mixtures with varied CO_2 mole fractions while at a fixed T = 333 K and a fixed P = 7.69 MPa. It is seen that the MSDs increase linearly with the elapse time Δt. Note that at high CO_2 mole fractions, the systems are locally phase-separated, which may result in inhomogeneous diffusion along different directions. However, our results show that the MSDs of CO_2 molecules along x, y, and z directions are nearly equivalent to each other and are one-third the magnitude of the total MSD (Figure S3) because the CO_2 and alkane distributions, on a macroscopic scale, are almost uniform along the three dimensions after the system sufficiently reached equilibrium.

From the slopes of the MSD curves, the diffusion coefficients of CO_2 and alkane molecules can be obtained according

$$D = \frac{\lim_{\Delta t \to \infty} \mathrm{MSD}(\Delta t)}{6\Delta t} \quad (5)$$

as shown in Table S1 and Figures 10 and 11. We find that at low CO_2 contents, the diffusion coefficients of both CO_2 and alkane molecules increase with CO_2 mole fraction only very slightly because, under that condition, the diffusion of CO_2 or an alkane is mainly controlled by the viscous drags of the surrounding alkane molecules. Cadogan et al.[47] and Moultos et al.[31] reported the diffusivity of infinitely diluted CO_2 in various alkanes, including hexane, octane, and decane, by experiments and simulations, respectively. They found that the CO_2 diffusivity is about 0.3×10^{-4} to 2×10^{-4} cm^2 s^{-1} depending on the alkane type, temperature, and pressure, which is of the same magnitude as that estimated from the present simulation study for the cases at low CO_2 mole fractions. When the CO_2 mole fraction exceeds a value of ~60%, the diffusivities of both CO_2 and alkane rise greatly, suggesting that the addition of increasingly more CO_2 molecules would promote the motion of both CO_2 and alkane molecules. This is because the insertion of a certain number of CO_2 molecules into the gap of alkane molecules would expand the space between alkane molecules and hence can reduce the space barriers of alkane molecules to CO_2 and the interaction between alkane molecules. This trend is extremely significant at CO_2 mole fractions >60% where the number of CO_2 molecules is dominant and the n-alkane molecules are spread among the CO_2 phases. As CO_2 molecules are smaller than alkane molecules, they can move faster than the alkane molecules.

Increasing the temperature would enhance the diffusivity of both CO_2 and alkane molecules, especially at high CO_2 contents (Figures 10a and 11a) due to the increase in molecular kinetic energy and the expansion of the system volume that allows much freer movement of molecules. However, the influence of pressure on diffusivity is very limited except when P = 8.67 MPa (Figures 10b and 11b). At P = 8.67 MPa and T = 333 K, CO_2 is in the supercritical state when the mobility of both CO_2 and alkane molecules increases significantly. With the increase in n-alkane chain length, the diffusivity of both CO_2 and alkane molecules decreases (Figures 10c and 11c) because the long alkane chains not only can reduce their own mobility but also would retard the transport of their surrounding CO_2 molecules.

4. CONCLUSIONS

We have performed atomistic MD simulations to investigate the density and volumetric behavior of three typical n-alkanes (hexane, octane, and decane) influenced by different mole fractions of CO_2 injected in them at temperatures from 303 to 363 K and pressures from 3.8 to 8.67 MPa. Our results indicate that at low CO_2 mole fractions, the CO_2 molecules are filled in the space between n-alkane molecules and completely dissolved in the liquid n-alkane, leading to only a slight swelling of the alkane. Since the increase amplitude of system volume is below that of mass, the system density increases. Due to poor compressibility of such systems, their density and volume are only slightly influenced by temperature and pressure. When the CO_2 mole fraction is higher than 60% or greater, the system splits into two separated phases, i.e., the CO_2-saturated alkane phase and the CO_2-dominated gas phase, resulting in the rapid expansion of volume and the reduction in density. For the two-phase simulated states, the large ratio of surface area to volume means that our results do not represent the real thermodynamic condition. Therefore, the results for

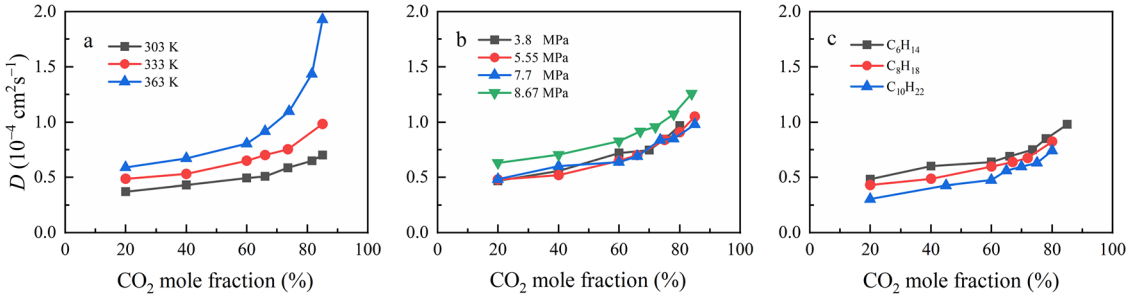

Figure 10. Diffusion coefficient (D) of CO_2 in a hexane/CO_2 mixture as a function of CO_2 mole fraction: (a) at a fixed P = 7.69 MPa but at different T values and (b) at a fixed T = 333 K but at different P values as indicated. (c) D of CO_2 in different n-alkane/CO_2 mixtures as a function of CO_2 mole fraction at P = 7.69 MPa and T = 333 K.

https://doi.org/10.1021/acsomega.1c03889
ACS Omega 2021, 6, 29618−29628

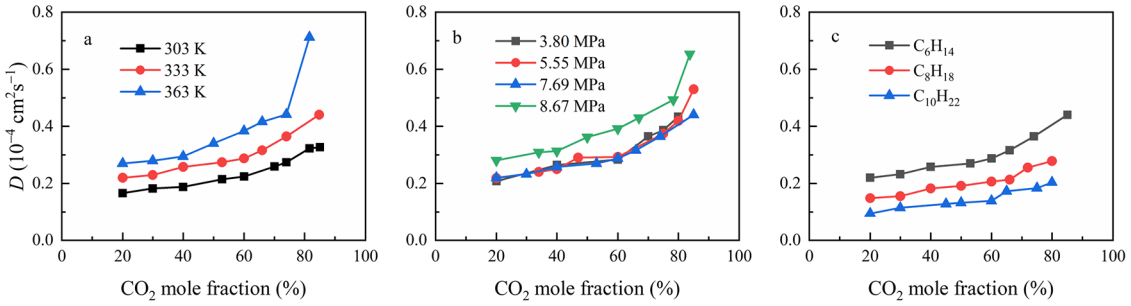

Figure 11. D of hexane molecules as a function of CO_2 mole fraction: (a) at a fixed P = 7.69 MPa but at different T values and (b) at a fixed T = 333 K but at different P values. (c) D of hexane, octane, and decane as a function of CO_2 mole fraction at P = 7.69 MPa and T = 333 K.

these states should not be taken as quantitative but only as indicating qualitative changes in the behavior of the system. Owing to the existence of a highly compressible gas phase, the system density and volume can more easily be changed by temperature and pressure. Since it is harder for alkanes with longer chains to separate from each other, the volume swelling decreases and the density increases with increasing carbon number of *n*-alkane chains. Furthermore, it was found that the increase in CO_2 mole fraction, temperature, and the decrease in alkane chain length would promote the diffusion of both CO_2 and alkane molecules. However, the influence of pressure on molecular diffusion is very limited except when P = 8.67 MPa and T = 333 K, where CO_2 is in the supercritical state. In that state, the molecular diffusivity significantly increases, although the structural properties do not change much. In general, this work provides insight into aspects of the carbon sequestration and oil recovery processes.

■ ASSOCIATED CONTENT

Supporting Information

The Supporting Information is available free of charge at https://pubs.acs.org/doi/10.1021/acsomega.1c03889.

Tabulated results for densities, specific volumes, and diffusion coefficients shown in Figures 2, 3, 10, and 11; additional figures for the system equilibrium process and the initial and final configurations; MSD of CO_2 molecules and its components along x, y, and z directions (PDF)

■ AUTHOR INFORMATION

Corresponding Authors

Yulong Chen − *College of Materials Science and Engineering, Zhejiang University of Technology, Hangzhou 310014, China*; orcid.org/0000-0002-5906-2738; Email: chenyulong@zjut.edu.cn

Junliang Wang − *College of Environment, Zhejiang University of Technology, Hangzhou 310014, China*; Email: upupwang@zjut.edu.cn

Authors

Youhui Wang − *College of Materials Science and Engineering, Zhejiang University of Technology, Hangzhou 310014, China*

Zhiyan Pan − *College of Environment, Zhejiang University of Technology, Hangzhou 310014, China*; orcid.org/0000-0002-1623-5133

Jun Liu − *Key Laboratory of Beijing City on Preparation and Processing of Novel Polymer Materials, Beijing University of Chemical Technology, Beijing 100029, China*

Complete contact information is available at: https://pubs.acs.org/10.1021/acsomega.1c03889

Notes

The authors declare no competing financial interest.

■ ACKNOWLEDGMENTS

This work was supported by the National Natural Science Foundation of China (41977304 and 51703198) and the National Key R&D Program of China (2019YFE0117200). Computations were performed at Tianhe-2, the National Supercomputer Center in Guangzhou, China.

■ REFERENCES

(1) Masson-Delmotte, V.; Zhai, P.; Pörtner, H.-O.; Roberts, D.; Skea, J.; Shukla, P. R.; Pirani, A.; Moufouma-Okia, W.; Péan, C.; Pidcock, R. Global warming of 1.5 °C. *An IPCC Special Report on the Impacts of Global Warming of 1.5 C* 2018, *1*, 1−9.

(2) Liu, S.; Ji, C.; Wang, C.; Chen, J.; Jin, Y.; Zou, Z.; Li, S.; Niu, S.; Zou, J. Climatic role of terrestrial ecosystem under elevated CO_2: A bottom-up greenhouse gases budget. *Ecol. Lett.* **2018**, *21*, 1108−1118.

(3) Aminu, M. D.; Nabavi, S. A.; Rochelle, C. A.; Manovic, V. A review of developments in carbon dioxide storage. *Appl. Energy* **2017**, *208*, 1389−1419.

(4) Huang, M.-T.; Zhai, P.-M. Achieving Paris agreement temperature goals requires carbon neutrality by middle century with far-reaching transitions in the whole society. *Adv. Clim. Chang. Res.* **2021**, *12*, 281−286.

(5) Bui, M.; Adjiman, C. S.; Bardow, A.; Anthony, E. J.; Boston, A.; Brown, S.; Fennell, P. S.; Fuss, S.; Galindo, A.; Hackett, L. A.; Hallett, J. P.; Herzog, H. J.; Jackson, G.; Kemper, J.; Krevor, S.; Maitland, G. C.; Matuszewski, M.; Metcalfe, I. S.; Petit, C.; Puxty, G.; Reimer, J.; Reiner, D. M.; Rubin, E. S.; Scott, S. A.; Shah, N.; Smit, B.; Trusler, J. P. M.; Webley, P.; Wilcox, J.; Mac Dowell, N. Carbon capture and storage (CCS): The way forward. *Energy Environ. Sci.* **2018**, *11*, 1062−1176.

(6) Chu, S. *Carbon capture and sequestration*. American Association for the Advancement of Science: 2009.

(7) Goeppert, A.; Czaun, M.; Prakash, G. K.; Olah, G. A. Air as the renewable carbon source of the future: An overview of CO_2 capture from the atmosphere. *Energy Environ. Sci.* **2012**, *5*, 7833−7853.

(8) Sanz-Pérez, E. S.; Murdock, C. R.; Didas, S. A.; Jones, C. W. Direct capture of CO_2 from ambient air. *Chem. Rev.* **2016**, *116*, 11840−11876.

(9) Zheng, J.; Chong, Z. R.; Qureshi, M. F.; Linga, P. Carbon dioxide sequestration via gas hydrates: a potential pathway toward decarbonization. *Energy Fuels* **2020**, *34*, 10529−10546.

(10) Godec, M. L.; Kuuskraa, V. A.; Dipietro, P. Opportunities for using anthropogenic CO_2 for enhanced oil recovery and CO_2 storage. *Energy Fuels* **2013**, *27*, 4183−4189.

(11) Menefee, A. H.; Ellis, B. R. Regional-scale greenhouse gas utilization strategies for enhanced shale oil recovery and carbon management. *Energy Fuels* **2020**, *34*, 6136−6147.
(12) Song, Z.; Li, Y.; Song, Y.; Bai, B.; Hou, J.; Song, K.; Jiang, A.; Su, S. In A Critical Review of CO_2 Enhanced Oil Recovery in Tight Oil Reservoirs of North America and China; *SPE/IATMI Asia Pacific Oil & Gas Conference and Exhibition*; OnePetro: 2020.
(13) Burrows, L. C.; Haeri, F.; Cvetic, P.; Sanguinito, S.; Shi, F.; Tapriyal, D.; Goodman, A.; Enick, R. M. A literature review of CO_2, natural gas, and water-based fluids for enhanced oil recovery in unconventional reservoirs. *Energy Fuels* **2020**, *34*, 5331−5380.
(14) Bachu, S.; Stewart, S. Geological sequestration of anthropogenic carbon dioxide in the western canada sedimentary basin: suitability analysis. *J. Can. Pet. Technol.* **2002**, *41*, PETSOC-02-02-01.
(15) Yang, Z.; Li, M.; Peng, B.; Lin, M.; Dong, Z. Dispersion property of CO_2 in oil. 1. Volume expansion of CO_2 + alkane at near critical and supercritical condition of CO_2. *J. Chem. Eng. Data* **2012**, *57*, 882−889.
(16) Han, H.; Yuan, S.; Li, S.; Liu, X.; Chen, X. Dissolving capacity and volume expansion of carbon dioxide in chain *n*-alkanes. *Pet. Explor. Dev.* **2015**, *42*, 97−103.
(17) Wang, J.; Zhou, S.; Bei, K.; Zhang, D.; Chou, I. M.; Chen, Z.; Lin, C.; Pan, Z. Using a fused silica capillary cell and in situ Raman spectroscopy to develop a setup for measurement of the volume expansion of carbon dioxide + *n*-hexane. *Energy Fuels* **2017**, *31*, 6314−6319.
(18) Wang, J.; Zhou, S.; Bei, K.; Chou, I. M.; Lin, C.; Pan, Z. A new approach for the measurement of the volume expansion of a CO_2 + *n*-dodecane mixture in a fused silica capillary cell by Raman spectroscopy. *Fuel* **2017**, *203*, 113−119.
(19) Bei, K.; Wang, J.; Zhou, S.; Xie, G.; Xu, Y.; Wang, L.; Jiang, Z.; Chou, I. M.; Pan, Z. Determining the volume expansion of the CO_2 + octane mixture using a fused silica capillary cell with in-situ Raman spectroscopy. *J. CO2 Util.* **2018**, *24*, 149−156.
(20) Hu, R.; Crawshaw, J. P.; Trusler, J. P. M.; Boek, E. S. Rheology and phase behavior of carbon dioxide and crude oil mixtures. *Energy Fuels* **2017**, *31*, 5776−5784.
(21) Zhang, Y.; Wang, L.; Liu, S.; Song, Y.; Liu, Y.; Jiang, L. Density and volumetric behavior of CO_2+ undecane system from 313. 15 to 353.15 K and pressures up to 19 MPa. *J. Chem. Eng. Data* **2016**, *61*, 3003−3012.
(22) Zhao, C.; Lu, D.; Chen, K.; Chi, Y.; Liu, S.; Yuan, L.; Zhang, Y.; Song, Y. Review of density measurements and predictions of CO_2−alkane solutions for enhancing oil recovery. *Energy Fuels* **2021**, *35*, 2914−2935.
(23) Galicia-Luna, L. A.; Pimentel-Rodas, A.; Castro-Arellano, J. J.; Notario-López, A. M.; Sánchez-García, C.; Esquivel-Mora, P. Twenty years of experimental determinations of thermophysical properties with high accuracy: Thermodynamics Laboratory, ESIQIE-IPN, México. *J. Chem. Eng. Data* **2019**, *64*, 2075−2083.
(24) Pereira, L. M. C.; Chapoy, A.; Burgass, R.; Tohidi, B. Measurement and modelling of high pressure density and interfacial tension of (gas + *n*-alkane) binary mixtures. *J. Chem. Thermodyn.* **2016**, *97*, 55−69.
(25) Zhang, Y.; Liu, Z.; Liu, W.; Zhao, J.; Yang, M.; Liu, Y.; Wang, D.; Song, Y. Measurement and modeling of the densities for CO_2 + dodecane system from 313.55 K to 353.55 K and pressures up to 18 MPa. *J. Chem. Eng. Data* **2014**, *59*, 3668−3676.
(26) Song, Y.; Jian, W.; Zhang, Y.; Shen, Y.; Zhan, Y.; Zhao, J.; Liu, Y.; Wang, D. Densities and volumetric characteristics of binary system of CO_2 + decane from (303.15 to 353.15) K and pressures up to 19 MPa. *J. Chem. Eng. Data* **2012**, *57*, 3399−3407.
(27) Zhang, Y.; Jian, W.; Song, Y.; Liu, W.; Yang, M.; Zhao, J.; Liu, Y.; Zhao, Y. (p, ρ, T) behavior of CO_2 + tetradecane systems: experiments and thermodynamic modeling. *J. Chem. Eng. Data* **2015**, *60*, 1476−1486.
(28) Zúñiga-Moreno, A.; Galicia-Luna, L. A.; Camacho-Camacho, L. E. Compressed liquid densities and excess volumes of CO_2 + decane mixtures from (313 to 363) K and pressures up to 25 MPa. *J. Chem. Eng. Data* **2005**, *50*, 1030−1037.
(29) Wang, B.; He, J.; Sun, D.; Zhang, R.; Han, B. Solubility of chlorobutane, ethyl methacrylate and trifluoroethyl acrylate in supercritical carbon dioxide. *Fluid Phase Equilib.* **2006**, *239*, 63−68.
(30) Tolley, W. K.; Izatt, R. M.; Oscarson, J. L. Simultaneous measurement of excess enthalpies and solution densities in a flow calorimeter. *Thermochim. Acta* **1991**, *181*, 127−141.
(31) Moultos, O. A.; Tsimpanogiannis, I. N.; Panagiotopoulos, A. Z.; Trusler, J. P. M.; Economou, I. G. Atomistic molecular dynamics simulations of carbon dioxide diffusivity in *n*-hexane, *n*-decane, *n*-hexadecane, cyclohexane, and squalane. *J. Phys. Chem. B* **2016**, *120*, 12890−12900.
(32) Zhang, J.; Seyyedi, M.; Clennell, M. B. Molecular dynamics simulation of transport and structural properties of CO_2−alkanes. *Energy Fuels* **2021**, *35*, 6700−6710.
(33) Zhang, J.; Pan, Z.; Liu, K.; Burke, N. Molecular simulation of CO_2 solubility and its effect on octane swelling. *Energy Fuels* **2013**, *27*, 2741−2747.
(34) Choudhary, N.; Che Ruslan, M. F. A.; Narayanan Nair, A. K.; Sun, S. Bulk and interfacial properties of alkanes in the presence of carbon dioxide, methane, and their mixture. *Ind. Eng. Chem. Res.* **2021**, *60*, 729−738.
(35) Yang, Y.; Narayanan Nair, A. K.; Anwari Che Ruslan, M. F.; Sun, S. Bulk and interfacial properties of the decane + water system in the presence of methane, carbon dioxide, and their mixture. *J. Phys. Chem. B* **2020**, *124*, 9556−9569.
(36) Mohammed, S.; Mansoori, G. A. The role of supercritical/dense CO_2 gas in altering aqueous/oil interfacial properties: A molecular dynamics study. *Energy Fuels* **2018**, *32*, 2095−2103.
(37) Makimura, D.; Kunieda, M.; Liang, Y.; Matsuoka, T.; Takahashi, S.; Okabe, H. Application of molecular simulations to CO_2-enhanced oil recovery: phase equilibria and interfacial phenomena. *SPE J.* **2013**, *18*, 319−330.
(38) Negahban, S.; Kazemi, M.; Kalantari, M.; Dindoruk, B.; Elshahawi, H. "Digital Fluid Physics:" Prediction of phase equilibria for several mixtures of CO_2 with petroleum fluid systems. *J. Pet. Sci. Eng.* **2020**, *187*, 106752.
(39) Liu, B.; Shi, J.; Sun, B.; Shen, Y.; Zhang, J.; Chen, X.; Wang, M. Molecular dynamics simulation on volume swelling of CO_2−alkane system. *Fuel* **2015**, *143*, 194−201.
(40) Li, C.; Pu, H.; Zhao, J. X. Molecular simulation study on the volume swelling and the viscosity reduction of *n*-alkane/CO_2 systems. *Ind. Eng. Chem. Res.* **2019**, *58*, 8871−8877.
(41) Sun, H. COMPASS: An ab initio force-field optimized for condensed-phase applications overview with details on alkane and benzene compounds. *J. Phys. Chem. B* **1998**, *102*, 7338−7364.
(42) Yang, J.; Ren, Y.; Tian, A. M.; Sun, H. COMPASS force field for 14 inorganic molecules, He, Ne, Ar, Kr, Xe, H_2, O_2, N_2, NO, CO, CO_2, NO_2, CS_2, and SO_2, in liquid phases. *J. Phys. Chem. B* **2000**, *104*, 4951−4957.
(43) Wu, G.; He, L.; Chen, D. Sorption and distribution of asphaltene, resin, aromatic and saturate fractions of heavy crude oil on quartz surface: molecular dynamic simulation. *Chemosphere* **2013**, *92*, 1465−1471.
(44) Zhao, L.; Lin, S.; Mendenhall, J. D.; Yuet, P. K.; Blankschtein, D. Molecular dynamics investigation of the various atomic force contributions to the interfacial tension at the supercritical CO_2−water interface. *J. Phys. Chem. B* **2011**, *115*, 6076−6087.
(45) Span, R.; Wagner, W. A new equation of state for carbon dioxide covering the fluid region from the triple-point temperature to 1100 K at pressures up to 800 MPa. *J. Phys. Chem. Ref. Data* **1996**, *25*, 1509−1596.
(46) Einstein, A. Über die von der molekularkinetischen Theorie der Wärme geforderte Bewegung von in ruhenden Flüssigkeiten suspendierten Teilchen. *Ann. Phys.* **1905**, *322*, 549−560.
(47) Cadogan, S. P.; Mistry, B.; Wong, Y.; Maitland, G. C.; Trusler, J. P. M. Diffusion coefficients of carbon dioxide in eight hydrocarbon

https://doi.org/10.1021/acsomega.1c03889
ACS Omega 2021, 6, 29618−29628

liquids at temperatures between (298.15 and 423.15) K at pressures up to 69 MPa. *J. Chem. Eng. Data* **2016**, *61*, 3922−3932.

https://doi.org/10.1021/acsomega.1c03889
ACS Omega 2021, 6, 29618−29628